Visualization of Single Molecules of RNA Polymerase Sliding along DNA

Hiroyuki Kabata, Osamu Kurosawa, Ichiro Arai, Masao Washizu, Stefanie A. Margarson, Robert E. Glass, Nobuo Shimamoto*

Transcription requires that RNA polymerase binds to promoters buried in nonspecific sites on DNA. The search for promoters may be facilitated if the polymerase slides along the molecule of DNA. Single molecules of *Escherichia coli* RNA polymerase were visualized, and their movements on immobilized bacteriophage λ and T7 DNAs were examined. Deviating from drifts by bulk flow, about 40 percent of the enzyme molecules moved along the extended DNA. The results provide direct evidence for sliding as a mechanism for relocation of the enzyme on DNA.

In addition to simple dissociation and association, two mechanisms—intersegment transfer and sliding—have been proposed for translocation of a protein molecule from one site on DNA to another (*1, 2*). The former is supported by the identification of an essential intermediate in which a protein oligomer makes contact with two separate sites on a DNA molecule (*3*). In contrast, only indirect evidence for the latter mechanism is available from kinetic studies of bacterial repressors (*1, 4, 5*), nucleases (*6*), a methylase (*7*), and DNA polymerases (*8*). Moreover, the presence of sliding was conflictingly concluded for a repressor (*4, 9*).

In the initiation of transcription, *E. coli* RNA polymerase holoenzyme (subunit composition of $\alpha_2\beta\beta'\sigma$) (*10*) binds to promoters on DNA; sliding has been suggested as a mechanism for promoter searching in kinetic studies (*11, 12*). We developed a visual examination for the putative sliding motion of a holoenzyme molecule. The principle of single-molecule dynamics has been successfully applied in the study of motor proteins (*13*).

To detect sliding as a linear movement, we extended DNA in a common orientation between aluminum electrodes on a glass slide by dielectrophoresis (*14*), forming "DNA belts" (Fig. 1A). The belts were retained after the electric field was cut off because the DNA molecule was anchored to the surface at both ends with avidin (Fig. 1B). The belt was 2 to 3 μm thick, with a concentration of 10 to 300 μg/ml (*15*). If the association rate constant of holoenzyme and immobilized DNA is 10^5 M^{-1} s^{-1}, as previously reported for free DNA (*12*), one binding event would require a residence time of 0.2 to 6.0 s in the DNA belt; this is quicker than the bleaching of fluorophore attached to holoenzyme as follows.

We visualized a single holoenzyme molecule by conjugating it with rhodamine-avidin (*16*) by means of the Fab fragment of immunoglobulin G (IgG) recognizing the COOH-terminus of the β′ subunit (*17*). The antibody is known to preserve the transcription activity of holoenzyme (*18*). The enzyme solution was injected between the cover slip and the slide so that 2 to 10 molecules of enzyme were detected at each injection in a single view covering 90-μm stretches of both DNA belts. Bulk flow occurred on injection and carried the protein molecules into the belt.

The observed movements were indistinguishable from random Brownian motion when bulk flow was slower than 0.5 μm/s. In the presence of faster bulk flow tilting relatively to the stretched DNA, the movements were classified into one of five characteristic modes: (i) translocation longer than 3 μm in parallel with the fixed DNA (±10°); (ii) vertical jumping more than 3 μm; (iii) translocation shorter than 2 μm for more than 10 s; (iv) translocation longer than 3 μm in parallel with bulk flow (±30°) and not classified into (i), (ii), or (iii); and (v) any others (Fig. 2).

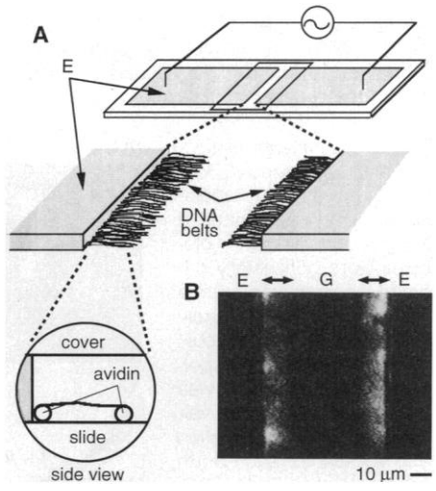

Fig. 1. DNA belts. (**A**) DNA was stretched in parallel by dielectrophoresis and (**inset**) fixed with the avidin molecules adsorbed onto the surface (*19*). (**B**) Fluorescence image of the λ DNA belts visualized with ethidium bromide after a few rounds of the assay. Electrodes (E) and glass surface (G) are denoted, and the DNA belts are indicated with dihedral arrows.

Most traces were mode (iv) either outside the DNA belt (Fig. 2A, left) or with bulk flow faster than 100 μm/s and were explained as a simple drift superimposed by Brownian motion. In contrast, modes (i) through (iii) were observed only in the belts with moderate bulk flow giving a residence time longer than 0.5 s (Fig. 2A, right). Moreover, these modes disappeared when the DNA binding site of holoenzyme was blocked with heparin or a free fragment of DNA and were not found in the movements of anti-β′ IgG possessing no DNA binding sites (Table 1). Therefore, the binding to the fixed DNA caused modes (i)

Table 1. Modes of movements in λ DNA belts and effects of heparin and a free DNA. Numbers of modes were counted for all traces in the belts with bulk flow rate of 1 to 20 μm/s. A trace containing modes (i) through (iii) was counted as each of the three even when it contained other modes. A trace containing only mode (iv) was counted as (iv), and that containing (iv) and (v) or just (v) was counted as (v). Holoenzyme labeled with Fab (30 pM) was preincubated at 37°C for 1 hour with 30 nM heparin or a 239–base pair DNA containing λ p_R at position 134.

Mode	Distribution (%)			
	E. coli RNA polymerase			anti-β′ IgG alone
	alone	heparin	free DNA	
(i) Sliding	39	2	13	4
(ii) Jumping	7	1	0	0
(iii) Promoter binding	6	2	1	0
(iv) Simple drift	20	79	66	86
(v) unidentified	28	16	22	10
Total number of samples	(148)	(132)	(203)	(247)

H. Kabata and N. Shimamoto, DNA Research Center, National Institute of Genetics, and School of Life Science, The Graduate University for Advanced Studies, Mishima, Japan 411.
O. Kurosawa, Department of Electrical Engineering and Electronics, Seikei University, and Advance Company, Tokyo, Japan 103.
I. Arai and M. Washizu, Department of Electrical Engineering and Electronics, Seikei University, Tokyo, Japan 103.
S. A. Margarson and R. E. Glass, Department of Biochemistry, Queen's Medical Center, Nottingham University, Nottingham, UK NG7 2UH.
*To whom correspondence should be addressed.

through (iii), and mode (i) may be sliding along DNA. The observed requirement of DNA binding activity excluded the alternative possibility that mode (i) was a drift following a bulk flow locally inflected by the DNA. Mode (i) was the most frequent mode with moderate flow, twice as frequent as the simple drift (Table 1), confirming sliding was a true activity of the enzyme.

Mode (ii) occurred near the electrode edges (Fig. 2, A and C) where a maximum of 15% of DNA was looped or vertically oriented (*15*). It may be explained as sliding along such nonparallel DNA. Mode (iii) tends to occur near the ends of T7 ΔD111 DNA (Fig. 2, D and E) or at a position one fourth of the length of λ DNA, consistent with the binding to the major promoters.

In Fig. 3, two enzyme molecules started sliding from putative promoters, drawing traces ending in mode (iii) near promoters in the other belt, suggesting sliding participates in promoter search. Interestingly, the velocities usually decreased during sliding (Fig. 3B), indicating friction between the enzyme and DNA. Such friction was masked by Brownian motion in case of slow flow (Fig. 2B). The two molecules in Fig. 3 changed their directions at different moments, again indicating sliding is not drifts following a bulk flow with changing directions. Therefore, sliding is a mechanism for relocation of the enzyme on DNA.

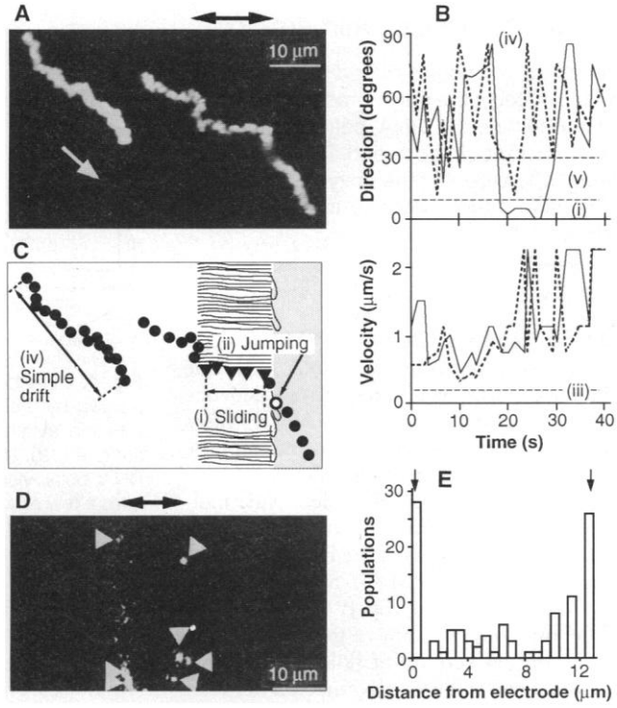

Fig. 2. Movements of fluorescently visualized *E. coli* RNA polymerase molecules. (**A**) Superimposed images. The λ DNA molecules were horizontally oriented as indicated with a dihedral arrow. White arrow shows the direction of bulk flow. The blurring of a spot, attributed to mode (ii), was also seen. (**B**) Absolute values of averaged direction and velocity for each 3-μm translocation. The DNA were fixed at 0°, and the modes are marked. The right molecule (solid line) but not the left (broken line) showed sliding in the belt. (**C**) Assignment of the movements. (**D**) Holoenzyme trapped on immobilized T7 ΔD111 DNA (dihedral arrow) is marked with white arrowheads. (**E**) Locations of 111 molecules in mode (iii) on T7 DNA. Arrows indicate the positions of T7A1 promoter.

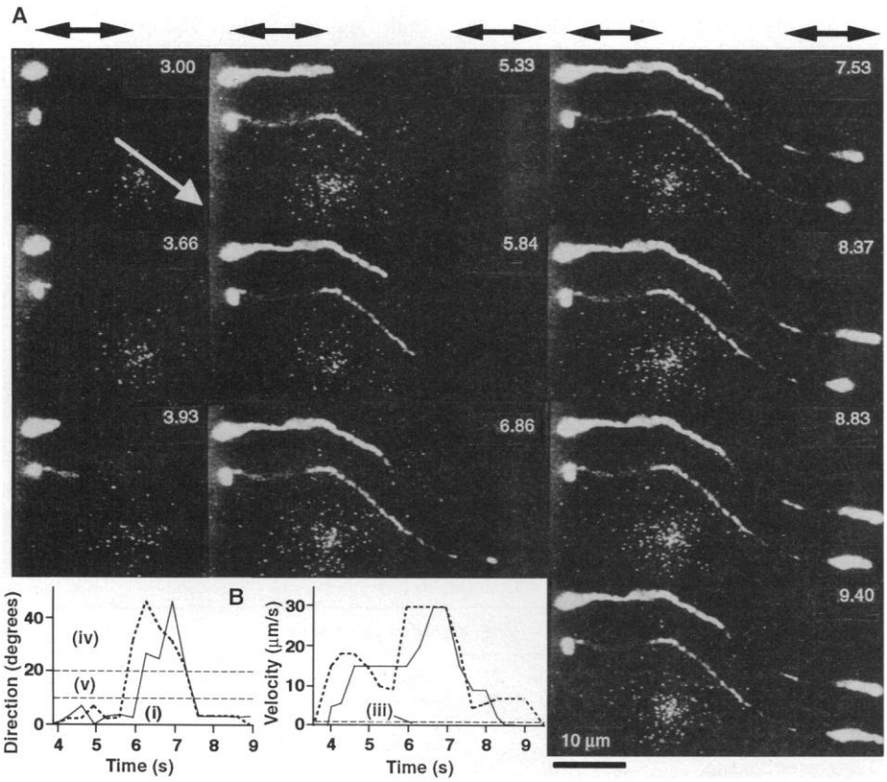

Fig. 3. Sliding movements in T7 DNA belts. (**A**) The images are superimposed until the time (in seconds) indicated in each panel. (**B**) Analysis of upper (solid line) and lower (broken line) traces similar to Fig. 2B.

REFERENCES AND NOTES

1. O. G. Berg, R. B. Winter, P. H. von Hippel, *Biochemistry* **20**, 6929 (1981).
2. P. H. von Hippel and O. G. Berg, *J. Biol. Chem.* **264**, 675 (1989).
3. A. Hochschild and M. Ptashne, *Cell* **44**, 681 (1986).
4. R. Ruusala and D. M. Crothers, *Proc. Natl. Acad. Sci. U.S.A.* **89**, 4903 (1992).
5. R. B. Winter and P. H. von Hippel, *Biochemistry* **20**, 6948 (1981); R. B. Winter, O. G. Berg, P. H. von Hippel, *ibid.*, p. 6961; J. G. Kim, Y. Takeda, B. W. Matthews, W. F. Anderson, *J. Mol. Biol.* **196**, 149 (1987).
6. H.-J. Ehbrecht, A. Pingoud, G. Urebenbake, G. Maass, C. Gualerzi, *J. Biol. Chem.* **260**, 6160 (1985); W. E. Jack, B. J. Terry, P. Modrich, *Proc. Natl. Acad. Sci. U.S.A.* **79**, 4010 (1982); B. J. Terry, W. E. Jack, R. A. Rubin, P. Modrich, *J. Biol. Chem.* **258**, 9820 (1983); B. J. Terry, W. E. Jack, P. Modrich, *ibid.* **260**, 13130 (1985); C. Nickell, M. A. Prince, R. S. Lloyd, *Biochemistry* **31**, 4189 (1992).
7. G. Nardone, J. George, J. G. Chirikjian, *J. Biol. Chem.* **261**, 12128 (1986).
8. P. T. Stukenberg, P. S. Studwell-Vaughan, M. O'Donnell, *ibid.* **266**, 11328 (1991); X.-P. Kong, R. Onrust, M. O'Donnell, J. Kuriyan, *Cell* **69**, 425 (1992); B. N. Beiinstev, S. K. Zavriev, M. F. Shemyakin, *Nucleic Acids Res.* **8**, 1391 (1980).
9. R. Fickert and B. Mueller-Hill, *J. Mol. Biol.* **226**, 59 (1992).
10. For example, R. R. Burgess, *Annu. Rev. Biochem.* **40**, 711 (1971).
11. M. Ricchetti, W. Metzger, H. Heumann, *Proc. Natl. Acad. Sci. U.S.A.* **85**, 4610 (1988); C. S. Park, Z. Hillel, C.-W. Wu, *J. Biol. Chem.* **257**, 6944 (1982); C. S. Park, F.-Y. Wu, C.-W. Wu, *ibid.*, p. 6950.
12. P. Singer and C.-W. Wu, *J. Biol. Chem.* **262**, 14178 (1987).
13. T. Yanagida, M. Nakase, K. Nishiyama, S. Oosawa, *Nature* **307**, 58 (1984); S. J. Kron and J. A. Spudich, *Proc. Natl. Acad. Sci. U.S.A.* **83**, 6272 (1986); R. D. Vale, T. S. Reese, M. P. Sheetz, *Cell* **42**, 39 (1985).
14. M. Washizu and O. Kurosawa, *IEEE Trans. Ind. Appl.* **26**, 1165 (1990).

15. The vertical distribution of the DNA in the belt was examined through a confocal microscope (Meridian Insight, Okemos MI).
16. N. Shimamoto, H. Kabata, O. Kurosawa, M. Washizu, in *Structural Tools for the Analysis of Protein–Nucleic Acid Complexes, Advances in Life Science*, D. M. J. Lilley, H. Heumann, D. Suck, Eds. (Birkhaeser Veerlag, Basel, Switzerland, (1992), p. 241. We introduced 10 to 40 molecules of rhodamine into an avidin tetramer.
17. Rabbit antibody was raised against COOH-terminus (22 amino acids) fused to β-galactosidase. Its Fab fragment [J. E. Coligan, A. M. Kruisbeek, D. H. Margulies, E. M. Shevach, W. Strober, in *Current Protocol in Immunology* (Wiley, New York, 1991), p. 2.8.1] was biotinylated [Instructions 20217X, Pierce] and coupled to a stoichiometric amount of rhodamine-avidin (*16*). Holoenzyme (*20*) was mixed with the labeled Fab and isolated through glycerol-gradient centrifugation [K. Igarashi, N. Fujita, A. Ishihama, *J. Mol. Biol.* **218**, 1 (1991)]. We used the immunolabeled enzyme (Fig. 2, Table 1) and chemically labeled enzyme (Fig. 3) (*16*). Samples on a plate maintained at 37°C were inspected through an Olympus RFLBHS microscope with a Hamamatsu C2400-08 camera.
18. S. A. Margarson and R. E. Glass, unpublished data.
19. A pair of aluminum electrodes with a gap of 80 to 100 μm was vacuum-deposited on a glass slide. Biotin was attached at both ends of T7 ΔD111 or λ*cI*857*S*am7 DNA (*20*), incubated with twice the stoichiometric amount of hen-egg avidin, and after dilution with water to give a 2 μg/ml DNA solution, 5 μl of the solution was placed near the electrode gap and covered with a cover slip. A 1-s pulse of 1 MHz at 20 kV/cm was applied at every 2 s for 10 to 30 min. The fixed DNA was washed with a working buffer [10 mM $MgCl_2$, 100 mM KCl, 0.1 mM dithiothreitol, tris-HCl (pH 8.0), and 0.4 mg of partially hydrolyzed casein per milliliter].
20. M. Fujioka, T. Hirata, N. Shimamoto, *Biochemistry* **30**, 1801 (1991).
21. We thank A. Ishihama, J. Tomizawa, and T. Yanagida for helpful discussions. Supported by grants from the Agency of Science and Technology of Japan and from the Ministry of Education, Science and Culture (N.S.) and by grants from the Medical Research Council, European Economic Commission, and British Council (R.E.G.).

16 July 1993; accepted 15 October 1993

Nucleosome Disruption by Transcription Factor Binding in Yeast

Randall H. Morse*

Studies in vivo and in vitro have shown that the packaging of DNA into chromatin can affect gene expression. Here, binding of the yeast transcriptional activator GAL4 to DNA in chromatin has been investigated in vivo with a yeast episome. A positioned nucleosome that is present in cells grown in glucose and contains a single GAL4 binding site is disrupted by GAL4 binding in galactose. GAL4 can also bind to DNA in chromatin when the carboxyl-terminal activation domain of GAL4 is either masked by GAL80 or is absent. These results show that a transcription factor can bind to its site in vivo in what would appear to be a repressive chromatin structure.

The incorporation of promoter elements into nucleosomes in vitro prevents transcription initiation, probably by occlusion or deformation of sequences recognized by specific trans-acting factors (*1*). Some factors, such as nuclear factor–1 (NF-1) and heat shock factor, do not bind well to nucleosomal DNA in vitro (*2*, *3*). However, other factors, such as the glucocorticoid receptor and GAL4, can bind and form ternary complexes with histone-bound DNA (*4*, *5*). The RNA polymerase III transcription factor TFIIIA can bind to a positioned nucleosome in vitro, but only when the histone NH_2-terminal regions are acetylated or absent (*6*).

Nucleosomes may also affect transcription initiation in vivo (*7*). In both the mouse mammary tumor virus promoter and the yeast *PHO5* gene, binding sites for transcriptional activators are located within positioned nucleosomes. In both cases, indirect evidence suggests that specific mechanisms are required to allow those factors access to their binding sites (*2*, *8*).

The well-characterized minichromosome TRP1ARS1 and its derivatives have been used to manipulate chromatin structure in yeast such that binding sites for trans-acting factors are included in or excluded from positioned nucleosomes (*9*–*11*). I have used this approach to investigate binding of the transcriptional activator GAL4 to its binding site when it is positioned within a nucleosome. A single copy of a near-consensus 17–base pair (bp) binding site for GAL4 was introduced into the DNA sequence normally located near the center of the stably positioned nucleosome I of a TRP1ARS1 derivative (*9*, *10*) to create the yeast episome TA17Δ80 (*12*). This plasmid was introduced into yeast cells, where it was maintained at >10 copies per cell. The chromatin structure of TA17Δ80 was assayed by the indirect end-label technique (*13*). In this technique, sites susceptible to micrococcal nuclease cleavage in chromatin and in naked DNA are mapped relative to a common restriction site. Regions that are protected in chromatin, but not in naked DNA, and which encompass 140 to 160 bp, are assumed to represent positioned nucleosomes (*9*).

When yeast cells harboring TA17Δ80 were grown in glucose, positioned nucleosomes were detected on the plasmid (Fig. 1, left panel, lanes labeled glucose). Nucleosome I contains the GAL4 binding site and is immediately adjacent to positioned nucleosome II. This structure was expected because GAL4 does not normally bind to its site in glucose, primarily because the *GAL4* gene is repressed (*14*). When cells harboring TA17Δ80 were grown in galactose, new micrococcal nuclease cleavage sites were observed in the nucleosome containing the GAL4 binding site, as well as in the neighboring nucleosome II (Fig. 1, left panel, lanes labeled galactose). This suggests that when cells harboring TA17Δ80 are grown in galactose, GAL4 is able to compete successfully with histones for occupancy of its binding site, resulting in the perturbation of a region of chromatin spanning two nucleosomes. This interpretation is supported by the finding that a control plasmid, TAΔ80, lacking the GAL4 binding site in nucleosome I, showed no change in the structure of this nucleosome between cells grown in glucose and galactose (Fig. 1, right panel). Nucleosome II appears less well positioned in TAΔ80 than in TA17Δ80, as evidenced by the incomplete protection of the cleavage in this region of TAΔ80; the reasons for this are not understood.

To determine whether GAL4 could activate transcription when its binding site is incorporated in a positioned nucleosome, I fused a 400-bp fragment encompassing nucleosomes I and II of TA17Δ80 to a β-galactosidase reporter gene (*15*). This construct, carried on a single-copy (CEN) plasmid, was introduced into yeast cells, which were assayed for β-galactosidase activity in the presence of glucose and galactose (Table 1). Activity was very low in glucose and strongly induced in galactose. The induced level of expression was not increased in the presence of a 2-μm-based plasmid containing the *GAL4* gene, indicating that maximal binding and transcription are achieved with normal wild-type levels of GAL4 protein. Micrococcal nuclease cleavage patterns of this plasmid were consistent with nucleosome I incorporating the same DNA sequence as in TA17Δ80 in cells grown in glucose; growth in galactose results in enhanced cleavage in this region (Fig. 2, arrow) as well as near the border of this

Laboratory of Cellular and Developmental Biology, National Institute of Diabetes and Digestive and Kidney Diseases, National Institutes of Health, Bethesda, MD 20892.

*Present address: Wadsworth Center for Laboratories & Research, Axelrod Institute, Post Office Box 12202, Albany, NY 11202.